



---

# A Model for Pheromone Discrimination in the Insect Antennal Lobe: Investigation of the Role of Neuronal Response Pattern Complexity

---

Christiane Linster<sup>1,2</sup> and Gérard Dreyfus<sup>1</sup>

<sup>1</sup>Laboratoire d'Électronique, École Supérieure de Physique et de Chimie Industrielles, 10, Rue Vauquelin, 75005 Paris, and <sup>2</sup>Laboratoire de Neurobiologie Comparée des Invertébrés, INRA/CNRS (URA 1190), 91140 Bures sur Yvette, France

Correspondence to be sent to: Christiane Linster, Department of Psychology (Rm 1446), Harvard University, 33 Kirkland Street, Cambridge, MA 02138, USA

---

## Abstract

Based on anatomical and physiological data pertaining to several moth species and the cockroach, we propose a neural model for pheromone discrimination in the insect antennal lobe. The model exploits the variety of neuronal response patterns observed in the macroglomerulus, and predicts how these complex patterns of excitation and inhibition can participate in the discrimination of the species-specific pheromone blend. The model also allows us to investigate the relationship between the distribution of observed response patterns and the neural organization from which these patterns emerge. *Chem. Senses* 21: 19–27, 1996.

## Introduction

One of the most striking features of neural olfactory processing and, in particular, olfactory processing in the insect antennal lobe, seems to be the variety of temporal response patterns (excitation versus inhibition) exhibited by olfactory neurons, and the variations of these patterns in response to stimulus quality (Sun *et al.*, 1993; Meredith, 1986). In this paper, we investigate how the response patterns of pheromone sensitive neurons in the insect antennal lobe can convey information about odor quality to higher order integration centers in the brain.

Temporal response patterns seem to be as important for olfactory pheromone processing in the specialist system as for the more complex odor processing tasks achieved by the generalist system, as it has been observed that '... the temporal patterns of these cells to presentation of the natural pheromone blend is clearly different than the responses to

each pheromone component presented alone, suggesting that these cells may act as feature detectors or, rather, mixture detectors. The summated response to the correct blend of pheromones might be qualitatively different from the responses to some other pheromone blend' (Christensen and Hildebrand, 1987b). The mechanisms by which the species-specific pheromone blend is discriminated are not elucidated and we propose here a modeling approach, based on anatomical and electrophysiological data, which shows how the temporal response patterns of antennal lobe neurons can contribute to the discrimination of the species-specific pheromone blend.

We recently proposed a model of the pheromone processing functional unit, the macroglomerular complex (MGC) in the male antennal lobe (Linster *et al.*, 1993a,b). We showed how a simple network model can reproduce a

number of features which have been described in the experimental literature. The response patterns observed in the model in reaction to simple and complex stimuli can be classified using the same criteria as those proposed for response patterns of olfactory neurons involved in the decoding of general odors in the insect antennal lobe (Sun *et al.*, 1993) and in the vertebrate olfactory bulb (Kauer, 1974; Meredith, 1986). Furthermore, we analytically derived the distribution of neuron response patterns as a function of the computer model parameters (Linster *et al.*, 1993c), and found, by simulation, the boundaries of regions in parameter space for which oscillatory responses occur (Linster, 1993). Although the model satisfactorily reproduced a number of experimental data, it was unable to account for pheromone discrimination at the antennal lobe level. We have also shown how neuronal oscillations can be used for pheromone ratio discrimination in a highly schematized model of the macroglomerulus (Linster *et al.*, 1994a,b). In the present paper, we show how the introduction of biological constraints, which had not been taken into account in the architecture of our previous models, allows us to propose a discrimination mechanism. No *ad hoc* hypotheses about the types of response patterns observed in the model are introduced; essentially, we further exploit the physiological data and the modeling data from the viewpoint of blend discrimination.

The central result of this study is the following: in the proposed model, stimulation by a blend of pheromone components in the species-specific concentration ratio results in a maximal number of complex response patterns (alternate phases of inhibition and excitation due to the same stimulation) conveyed from the antennal lobe to higher centers in the brain (e.g. the protocerebrum).

## Biological background

We use data pertaining to several moth species and to the cockroach. A number of points which are common to those species and which are relevant to our modeling approach are summarized below.

(1) In those species which have been studied, the blend is distinguishable not only by the nature of its components, but also by their precise concentration ratio (Kaissling and Kramer, 1990), which is not replicated in other species. This might facilitate the reproductive isolation between two or more sympatric species which share similar activity cycles and use the same pheromone components in different ratios.

The motivation of the present paper is to propose a possible mechanism for the discrimination of the concentration ratio.

The next five points are taken into account in the very design of our model.

(2) Most sexual pheromones are two- or multicomponent stimuli (Kaissling, 1987); for each component there is a separate receptor cell type, and non-overlapping molecular spectra (Boeckh and Selsam, 1984; Christensen *et al.*, 1987a).

(3) The axons of the pheromone specialist receptor cells project into a specific part of the antennal lobe: the macroglomerular complex (MGC) [for a review see (Masson and Mustaparta, 1990)].

(4) In some species there is evidence that functional specialization exists within MGC regions: physiologically distinct types of receptor cells project into different regions of the MGC (Hansson *et al.*, 1992). Antennal lobe neurons which respond preferentially to one component and not to the other can often be distinguished by extensive dendritic arborizations in sub-regions of the MGC (Boeckh and Selsam, 1984; Hösl, 1990; Kanzaki *et al.*, 1989).

(5) In the MGC, two types of antennal lobe neurons process pheromonal information: local interneurons (which have arborizations restricted to the antennal lobe) and projection (or output, relay) neurons, whose axons project to higher order processing centers. Antennal lobe neurons typically exhibit action potentials (Christensen and Hildebrand, 1987a; Masson and Mustaparta, 1990).

(6) Synaptic interaction in the MGC includes connections of primary afferent cells with local interneurons, as well as synaptic contacts between antennal lobe neurons (local interneurons and projection neurons) (Malun, 1991). Local interneurons seem to be responsible for most of the inhibitory synaptic activity (Christensen and Hildebrand, 1987b), and polysynaptic pathways between primary afferent and projection neurons (also via excitatory interneurons) seem to be the rule in the moth (Olberg, 1993; Christensen and Hildebrand, 1989b), and in the cockroach as well (Boeckh *et al.*, 1989; Distler, 1990).

Finally, the simulations of our models are in agreement with the next two experimental observations.

(7) Based on their electrophysiological responses to pheromone stimulation, three classes of antennal lobe interneurons and projection neurons can be distinguished in the MGC: (i) neurons which respond preferentially to one component but not to the other; (ii) neurons which respond in a similar fashion both to single components and to the blend; and (iii) neurons which show qualitatively different responses to

stimulation with one component or another, and with the blend (Burrows *et al.*, 1982; Olberg, 1983; Christensen and Hildebrand, 1987b; Christensen *et al.*, 1987b, 1989). Neurons of the third class respond with inhibition to one component, with excitation to the other, and with a mixed response of inhibition and excitation to the presentation of the blend.

(8) In the moth, neurons which receive mixed input from the two receptor cell types have been shown to follow pulsed stimulation up to a cut-off frequency: blocking of GABA diminishes this behavior by reducing the inhibitory phase of the response pattern (Christensen and Hildebrand, 1988; Christensen *et al.*, 1989b).

## Simulations

On the basis of experimental facts (2)–(6) summarized above, we build and simulate a model with simple neural elements (Figure 1), whose connectivity is random, but constrained by anatomical data:

- (1) constraint 1: we consider a blend of two components A and B; two groups of receptor cells  $R_A$  and  $R_B$ , sensitive to components A and B, respectively, project into functionally different layers  $L_A$  and  $L_B$  of local interneurons;
- (2) constraint 2: each local interneuron has a dense dendritic arborization in one of these areas, and a sparse arborization in the other;
- (3) constraint 3: projection neurons may receive input from all interneurons, but no direct afferent input from receptor cells.

The modeled neural elements are discrete time probabilistic neurons with memory which have been described in detail in previous models (Linster *et al.*, 1993a); equations and parameter values are given in the appendix.

A network is defined by the following parameters:

- (1) the number of local interneurons  $N$  and the number of projection neurons  $N_p$ ;
- (2) the probability  $n_i$  that a given interneuron is inhibitory; the probability that it is excitatory is  $n_e = 1 - n_i$ ;
- (3) the probability  $P_{Ai}$  that a connection exists between a given inhibitory interneuron and a receptor cell sensitive to A, and the probability  $P_{Bi}$  that a connection exists between a given inhibitory interneuron and a receptor cell sensitive to B; complying with constraint 1, one

has  $P_{Ai} = 1 - P_{Bi}$ ; probabilities  $P_{Ae}$  and  $P_{Be}$  are similarly defined, with  $P_{Ae} = 1 - P_{Be}$ ;

- (4) the connectivity  $c$ , which is the probability that a connection exists between any two interneurons; it was shown in (Linster *et al.*, 1993c) that the connectivity must be sparse in order for the full variety of responses to be observed;
- (5) the probability  $c_p$  that a connection exists between a given interneuron and a given projection neuron.

Therefore, the number of excitatory interneurons in layer  $L_A$  is a binomially distributed random variable with expectation value  $N_{Ai} = N n_i P_{Ai}$  and variance  $N n_i P_{Ai} (1 - n_i P_{Ai})$ . Similarly, one has:

$$N_{Ae} = N n_e P_{Ae} \text{ (expectation value of the number of excitatory interneurons in layer } L_A\text{),}$$

$$N_{Be} = N n_e P_{Be} \text{ (expectation value of the number of excitatory interneurons in layer } L_B\text{),}$$

$$N_{Bi} = N n_i P_{Bi} \text{ (expectation value of the number of inhibitory interneurons in layer } L_B\text{),}$$

with  $n_i = 1 - n_e$ ,  $P_{Ai} = 1 - P_{Bi}$  and  $P_{Ae} = 1 - P_{Be}$ .

If we make the simplifying approximation that the number of excitatory and inhibitory interneurons in each layer is equal to its expectation value, the number of connections that each projection neuron receives from the excitatory interneurons of layer  $L_A$  can be estimated as being  $N_{Ae} c_p$ ; similarly, it receives approximately  $N_{Ai} c_p$  connections from inhibitory interneurons of layer  $L_A$ ,  $N_{Be} c_p$  connections from excitatory interneurons of layer  $L_B$ , and  $N_{Bi} c_p$  connections from inhibitory interneurons of layer  $L_B$ .

All simulations presented in this paper were performed with  $n_i = 0.7$  (thus  $n_e = 0.3$ ),  $c = 0.1$  and  $c_p = 0.5$ .

Each network realization was obtained as follows:

- (1) parameters  $n$  and  $N_p$  were chosen;
- (2) for each interneuron, a realization  $r$  of a pseudo-random variable with uniform distribution in  $[0,1]$  was generated; if  $r < n_i$ , the neuron was considered as inhibitory, otherwise it was excitatory;
- (3) for each inhibitory interneuron, a realization  $r$  of a pseudo-random variable with uniform distribution in  $[0,1]$  was generated; if  $r < P_{Ai}$ , a connection was made from  $R_A$ , otherwise it was made from  $R_B$ ; a similar procedure was used for each excitatory interneuron;

- (4) for each pair of interneurons, a connection was made between them with probability  $c$ , using a similar procedure;
- (5) for each pair made of one interneuron and one projection neuron, a connection was made with probability  $c_p$ , using a similar procedure; no direct afference from receptor cell to projection neuron was made (constraint 3).

In order to obtain statistically significant results, we generated 200 network realizations for each set of parameters  $\{N, N_p, P_{Ai}, P_{Ae}\}$ ; each realization was simulated, and the responses of the interneurons and projection neurons to various stimulations (which will be detailed below) were

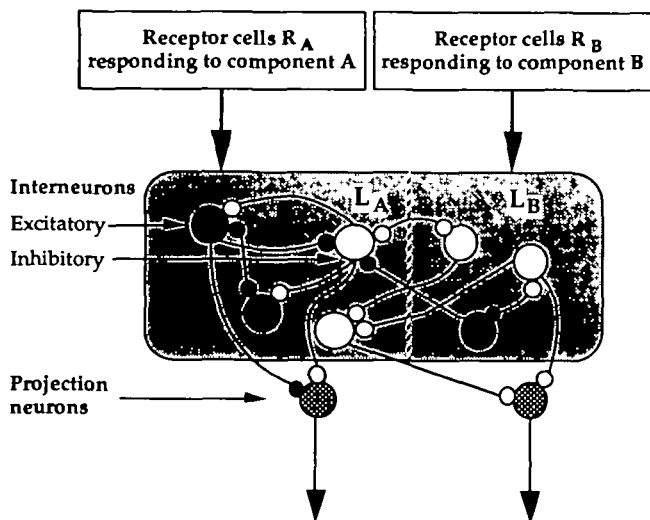


**Figure 1** Model architecture: the projection of receptor cells onto interneurons is constrained: interneurons may receive afferent synapses from one type of receptor cell (sensitive to input A or input B) only. Projection neurons do not receive direct afferent input from the receptor cells; it is their response which carries the output from the MGC to higher order integration centers in the brain. The connectivity between interneurons is sparse.

stored. Since we are interested in the distribution of response patterns, we designed an automatic classifier which assigned each response to one of four pattern classes: pure excitation, pure inhibition, mixed responses (alternate phases of excitation and inhibition) and non-response (the activity during stimulation differed from spontaneous activity by less than 10%). Examples of responses belonging to the first three classes are shown on Figure 2 (which will be described in more detail below). The classifier performed pairwise linear separation of the classes; since there are four classes, the classifier features six pairwise linear separators, trained by the Perceptron rule with the Pocket algorithm (Gallant, 1986); a detailed description of the classifier can be found in (Linster, 1993).

Each realization was submitted to stimulations with varying input ratios (A/B) with constant total amplitude  $A + B = 6$ ; for each stimulation, the response pattern of each projection neuron was classified and the frequency of occurrence of each class was computed; finally, the frequency of each response pattern class to a given stimulation was averaged over the 200 network realizations.

## Results

The results described in this section show that response pattern distributions vary with input ratio; hence, they can be used as representations of the composition of the blend. It can easily be shown that networks with identical layers  $L_A$  and  $L_B$  cannot discriminate whether input A or input B is dominant, because, on the average, projection neurons receive the same signal from input A and from input B, via local interneurons (Linster, 1993). It is therefore necessary to introduce a more specific connectivity in order to tune the model to a particular ratio or to a range of input ratios ( $A > B$ ) or ( $B > A$ ). We break the symmetry of the network

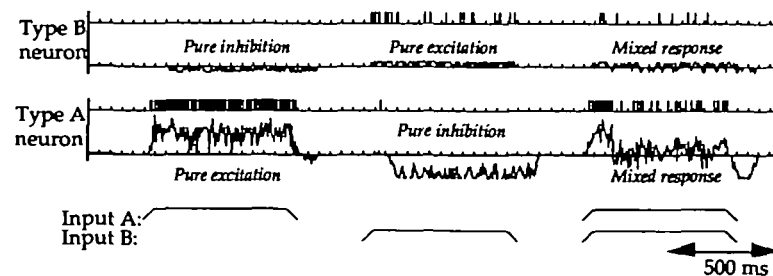


**Figure 2** Responses of two projection neurons to stimulation with A alone, B alone and ( $B = A$ ) in a non-symmetric network. The top two lines show the action potentials and the membrane potentials of a type B projection neuron (excited by B); the bottom two lines show the action potentials and the membrane potential of a type A projection neuron (excited by A).  $N = 63$ ,  $N_p = 7$  ( $N_{Ai} = 3.1$ ,  $N_{Ae} = 17.6$ ,  $N_{Be} = 1.3$ ,  $N_{Bi} = 41$ ).

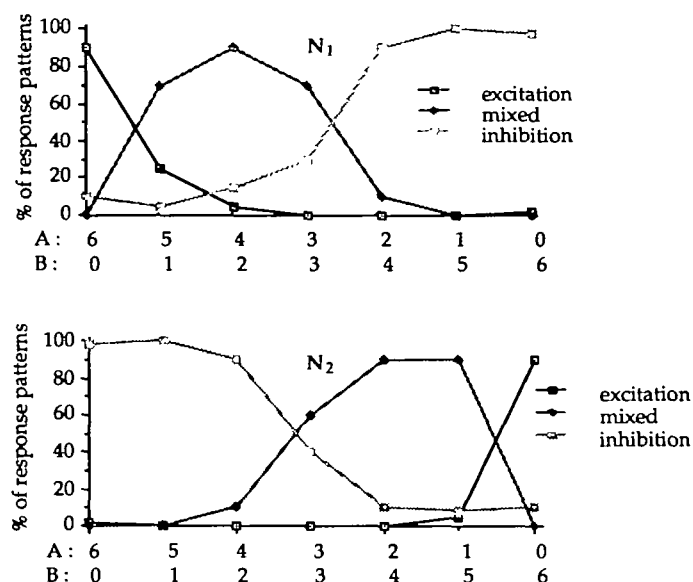


**Figure 3** Relative frequencies of projection neuron response patterns as a function of the input ratio  $A/B$  for network realizations with two parameter sets.  $N = 63$ ,  $N_p = 7$  (a)  $P_{Ai} = 0.07$  ( $N_{Ai} = 3.1$ ,  $N_{Ae} = 17.6$ ,  $N_{Be} = 1.3$ ,  $N_{Bi} = 41$ ) (b)  $P_{Ai} = 0.93$  ( $N_{Ai} = 41$ ,  $N_{Ae} = 1.3$ ,  $N_{Be} = 17.6$ ,  $N_{Bi} = 3.1$ )

by changing the probabilities that a receptor cell of a given type connects to an inhibitory (respectively excitatory) interneuron<sup>1</sup>, i.e. by assigning unequal values to  $P_{Ai}$  and  $P_{Ae}$ . For simplicity, we consider in all the following that  $P_{Ai} = P_{Be}$  and that  $P_{Ae} = P_{Bi}$ ; since  $P_{Ai} = 1 - P_{Bi}$  and  $P_{Ae} = 1 - P_{Be}$ , one has  $P_{Ai} = 1 - P_{Ae}$ . By so doing, we allow the dissymmetry of the network to be characterized by one single figure  $P_{Ai}$ : networks with  $P_{Ai} = 0.5$  are symmetrical, whereas networks with  $P_{Ai} = 0$  or  $P_{Ai} = 1$  have maximal dissymmetry.

## Response patterns

Figure 2 shows that, in agreement with observation (7) of the biological background, interneurons and projection neurons may exhibit qualitatively different responses to stimulations with one component, with the other, or with the blend. In the simulation shown, stimulations are performed by component A alone, by component B alone, and simultaneously by both components in equal concentrations; in order to exhibit the phenomena clearly, the network was made very asymmetrical:  $P_{Ai} = 0.07$  (hence,  $P_{Ae} = 0.93$ ), so that approximately 93% of all excitatory interneurons are in  $L_A$ , while 93% of all inhibitory interneurons are in  $L_B$

<sup>1</sup>Symmetry breaking can be achieved by other ways, such as introducing different stimulus/response curves for the receptor cell types (Linster, 1993).

(the choice of the value of  $P_{Ai}$  is purely illustrative and is not related to any biological data). The ‘type B’ neuron shown exhibits weak inhibition by component A, weak excitation by component B, and a mixed response to a stimulation by A and B simultaneously. The ‘type A’ neuron responds with strong excitation to A, is strongly inhibited by B, and responds with a strong excitation followed by a weaker excitation and a strong hyperpolarization (mixed response) to the simultaneous presentation by A and B.

## Distribution of response patterns: representation of the blend composition

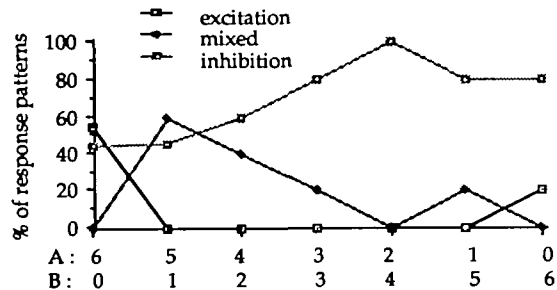
For illustration purposes, we consider a set  $N_1$  of network realizations with  $P_{Ai} = 0.07$  and a set  $N_2$  of networks with  $P_{Ai} = 0.93$ ; hence, in networks  $N_1$ , 93% of excitatory interneurons are in  $L_A$ , while 93% of inhibitory interneurons are in  $L_B$ . Therefore, the projection neurons of networks  $N_1$  receive mainly excitatory inputs from interneurons connected to receptor cells  $R_A$ , and mainly inhibitory inputs from interneurons connected to receptor cells  $R_B$ . It may be conjectured that the maximum number of mixed responses occur for blend compositions such that the excitation (coming essentially from layer  $L_A$ ) is equal to the inhibition (coming essentially from layer  $L_B$ ). Neglecting the small proportion of minority interneurons in both layers, and assuming that all neurons operate below their saturation threshold, the maximum frequency of mixed responses can be predicted to occur when  $n_{Ae} A \cong n_{Bi} B$ , where A and B stand for the concentrations in components A and B, respectively.

Figure 3a ( $N_1$ ) and Figure 3b ( $N_2$ ) show the relative frequencies of response patterns of projection neurons for a range of input stimulations ( $A/B$ ). The number of mixed responses is maximal for a given ratio ( $A > B$ ) in Figure 3a or ( $B > A$ ) in Figure 3b. From the above approximate argument, it can be predicted that the maximal number of mixed responses, for the set of parameters chosen, occurs for  $A = 5.1$  and  $B = 0.9$  for networks of  $N_1$ , and for  $A = 0.9$  and  $B = 5.1$  for networks of  $N_2$ . The results presented on Figure 3a and 3b are in qualitative agreement with the predictions.

In order to clarify and to illustrate the above considerations, we now analyse in detail the neuronal responses of networks with a specific set of parameters. We chose a set of parameters leading to a maximal number of complex response patterns of the projection neurons for input stimulation with  $A/B = 3/5$  (Figure 4 shows the relative frequencies of projection neuron response pattern as a function of varying input ratios). The average numbers of response patterns



observed in response to stimulation with pure and mixed components are in good accordance with physiological data (Christensen and Hildebrand, 1987a,b; 1988; Christensen *et al.*, 1989). In the network realizations with this set of parameters, on the average 85% of the excitatory and 15% of the inhibitory LNs receive input from  $R_A$ . Most projection neurons in these networks respond with excitation to input A and with inhibition to input B; these neurons respond with a mixed response of excitation and inhibition to the simultaneous presentation of A and B with  $A/B = 5/1$ . Few projection neurons respond with inhibition to input A and with excitation to input B; these neurons are inhibited in response to the simultaneous presentation of A and B with  $A/B = 5/1$ . However, the latter do respond to stimulation with  $A/B = 1/5$ .



**Figure 4** Relative frequencies of projection neuron response patterns for varying stimulation ratios  $A/B$  in the model MGC described in the text. Mixed responses reach a maximum value for input ratios 5/1. Stimulation with A leads to 50% excited and 50% inhibited responses. Stimulation with B alone inhibits 80% of the projection neurons.  $N = 29$ ,  $N_p = 6$ ,  $P_{Ai} = 0.15$ ,  $P_{Be} = 0.15$ ,  $P_{Bi} = P_{Ae} = 0.85$ ,  $N_{Ai} = 3.0$ ,  $N_{Ae} = 7.4$ ,  $N_{Be} = 1.3$ ,  $N_{Bi} = 17.3$ .

Figure 5 shows the responses of two selected projection neurons to pulsed stimulation at 5 Hz, with varying ratios  $A/B$ . Type A projection neurons respond with pure excitation to stimulation with A, but cannot follow the pulsed stimulation with excitatory bursts. For a range of inputs  $A > B$ , these neurons exhibit mixed responses, and they can follow the 5 Hz stimulation, responding to each stimulus pulse with a brief excitatory burst followed by an inhibitory phase. These neurons are inhibited as B increases. Type B projection neurons are inhibited when  $A > B$ . If A and B are almost equal, they respond with a brief excitatory burst followed by a long inhibitory phase; we observe in Figure 5 that they cannot follow pulsed stimulation.

For comparison purposes, we show in Figure 6 a classification, proposed by Christensen *et al.* (1989), for antennal lobe neurons in *Manduca sexta*. These studies use two synthetic compounds to mimic the constituents of the pheromone blend: *bombycal* (BAL), the ‘major’ pheromone component in *M. sexta* and (E,Z)-11,13-pentacadienal (C15), a mimic of a second *Manduca* pheromone component (Christensen and Hildebrand, 1987). ‘Pheromone generalists’ respond to both pheromone components by either excitation or inhibition; they cannot distinguish between the components and they cannot follow pulsed stimulation. ‘Pheromone specialists’ either respond to only one component and not to the other, or they respond by excitation to one component, by inhibition to the other and by a mixed response to the blend. These neurons respond with qualitatively different response patterns to the components and to the blend, and they can detect temporal changes in the stimulus. In the

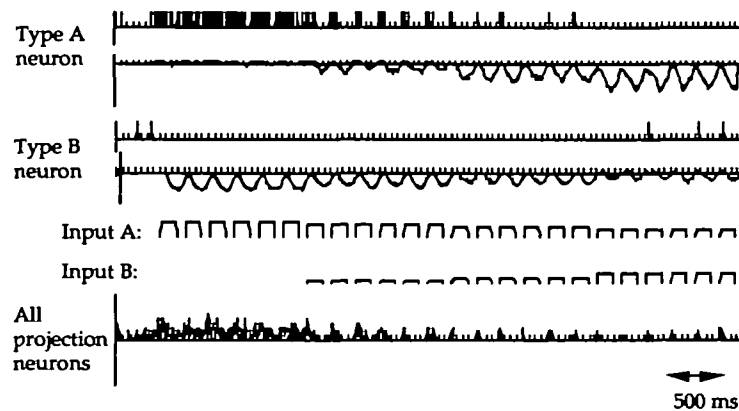


**Figure 5** Action potentials and membrane potential fluctuations in response to pulsed stimulation at 5 Hz with varying input ratio  $A/B$ . The figure shows the responses of two typical projection neurons in a network realization with the response pattern distribution shown in Figure 5. The first two traces show the action potentials and the membrane potential of a type A projection neuron. The next traces show the action potentials and the membrane potential of a type B projection neuron. The bottom trace shows the stimulation, below is shown the average activity and the average membrane potential of all projection neurons in this stimulation.  $N = 29$ ,  $N_p = 6$  ( $P_{Be} = 0.15$ ,  $P_{Bi} = P_{Ae} = 0.85$ ,  $N_{Ai} = 3.0$ ,  $N_{Ae} = 7.4$ ,  $N_{Be} = 1.3$ ,  $N_{Bi} = 17.3$ ).

## I. PHEROMONE GENERALISTS

## A. Cannot Discriminate Single Odors AND Cannot Code Temporal Changes

## 1. Excited Type

Stimulus : Response

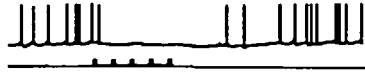
BAL	+
C15	+
Blend	+



## 2. Inhibited Type

Stimulus : Response

BAL	-
C15	-
Blend	-

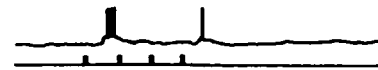


## II. PHEROMONE SPECIALISTS

## A. Can Discriminate Single Odors BUT Cannot Code Temporal Changes

Stimulus : Response

		(1) OR (2)
BAL	+	0
C15	0	+
Blend	+	+



## B. Can Discriminate Single Odors AND Can Code Temporal Changes

Stimulus : Response

		(1) OR (2)
BAL	+	-
C15	-	+
Blend	-	+



**Figure 6** Three types of pheromone sensitive antennal lobe neurons in *Manduca sexta*. Courtesy of T. Christensen and J. Hildebrand, from: Christensen *et al.*, 1989.

model, projection neurons which can be termed ‘pheromone generalists’ can be found for all types of stimuli, but they cannot follow pulsed stimulation. Neurons which can be termed ‘pheromone specialists’, however, are only active as a response to the species-specific ratio of components (this ratio depends on the ratio of inhibition and excitation in the interneuronal regions of the MGC). The mean output of the MGC can follow pulsed stimulation only if it is delivered at the corresponding ratio.

## Discussion

The model of the macroglomerular complex in insects, presented here, is based on a number of biological data and on previous modeling; it proposes a detailed mechanism of pheromone ratio discrimination and shows how the processing capabilities of a simple network can be exploited for ratio discrimination by an elementary breaking of symmetry. In our approach, stimulation by the species-specific ratio of pheromone component concentrations results in a

maximal number of complex temporal response patterns (alternate phases of excitation and inhibition) conveyed from the MGC to higher integration centers. In the model, we show that these temporal response patterns discriminate the species-specific blend from other blends (to our knowledge, this hypothesis has not been tested electrophysiologically). The pure, long-lasting excitation due to the major component alone, could lead, in higher order center neurons, to adaptation and fatigue, which would not occur for mixed responses, including periods of quiescence of projection neurons arising from the inhibitory signals resulting from the minor component.

Furthermore, projection neurons in the model can follow pulsed stimulation only if the species-specific blend is presented; this adds redundancy and stability to the system. Pulsed stimulation with single components or other ratios of the components cannot be followed with excitation bursts by these projection neurons.

These results are in good agreement with electrophysiological and behavioral data obtained on moths: pulsed stimula-

tion corresponds to the natural stimulus situation of at least some moth species, in which the female releases the pheromone blend not in a continuous, but in a rhythmic fashion (Baker *et al.*, 1985). In behavioural studies, meaningful behavior can only be obtained by pulsed stimulus presentation in male moths of these species. In addition, in some moth species, the ability to follow a range of pulse frequencies is strongest in those MGC neurons that can integrate information about both components of the pheromone blend (Christensen *et al.*, 1989; Linn *et al.*, 1987).

## ACKNOWLEDGEMENTS

The authors are grateful to L. Personnaz, C. Masson, M. Kerszberg and T. Christensen for fruitful discussions. C. Linster has been supported by a research grant (BFR91/05) from the Ministère des Affaires Culturelles, Grand-Duché de Luxembourg.

## REFERENCES

- Baker, T.C., Willis, M.A., Haynes, K.F. and Phelan, P.L. (1985) A pulsed cloud of sex pheromones elicits upwind flight in male moths. *Physiol. Entomol.*, **10**, 257–265.
- Boeckh, J. and Selsam, P. (1984) Quantitative investigation of the odor specificity of central olfactory neurons in the American cockroach. *Chem. Senses*, **9**, 396–380.
- Boeckh, J., Ernst, K.D. and Selsam, P. (1989) Double labelling reveals monosynaptic connections between antennal receptor cells and identified interneurons of the deutocerebrum in the American cockroach. *Zool. Jb. Anat.*, **119**, 303–312.
- Burrows, M., Boeckh, J. and Esslen, J. (1982) Physiological and morphological properties of interneurons in the deutocerebrum of male cockroaches which respond to female pheromones. *J. Comp. Physiol.*, **145**, 447–457.
- Christensen, T.A. and Hildebrand, J.G. (1987a) Functions, organization, and physiology of the olfactory pathways in the lepidopteran brain. In Gupta, A.P. (ed.), *Arthropod Brain: its Evolution, Development, Structure and Functions*. John Wiley & Sons, Harlow.
- Christensen, T.A. and Hildebrand, J.G. (1987b) Male-specific, sex pheromone-selective projection neurons in the antennal lobes of the moth. *Manduca sexta*. *J. Comp. Physiol. A*, **160**, 553–569.
- Christensen, T.A. and Hildebrand, J.G. (1988) Frequency coding by central olfactory neurons in the spinx moth *Manduca sexta*. *Chem. Senses*, **13**, 123–130.
- Christensen, T.A., Mustaparta, H. and Hildebrand, J.G. (1989) Discrimination of sex pheromone blends in the olfactory system of the moth. *Chem. Senses*, **14**, 463–477.
- Distler, P. (1990) GABA-immunohistochemistry as a label for identifying types of local interneurons and their synaptic contacts in the antennal lobe of the American cockroach. *Histochemistry*, **93**, 617–626.
- Gallant, S.I. (1986) Three constructive algorithms for network training. *Proc. Eight Ann. Conf. Cognitive Sci. Soc.*, 652–660.
- Hansson, B., Ljungberg, H., Hallberg, E. and Löfstedt, C. (1992) Functional specialization of olfactory glomeruli in a moth. *Science*, **256**, 1313–1315.
- Hösl, M. (1990) Pheromone-sensitive neurons in the deutocerebrum of *Periplaneta americana*: receptive fields on the antenna. *J. Comp. Physiol. A*, **167**, 321–327.
- Kaisling, K.-E. (1987) *R.H. Wright Lectures on Insect Olfaction*. Simon Fraser University, Burnaby, Canada.
- Kaisling, K.-E. and Kramer, E. (1990) Sensory basis of pheromone-mediated orientation in moths. *Verh. Dtsch. Zool. Ges.*, **83**, 109–131.
- Kanzaki, R., Arbas, E.A., Strausfeld, N.J. and Hildebrand, J.G. (1989) Physiology and morphology of projection neurons in the antennal lobe of the male moth *Manduca sexta*. *J. Comp. Physiol. A*, **165**, 427–453.
- Kauer, J.S. (1974) Response patterns of amphibian olfactory bulb neurons to odor stimulation. *J. Physiol.*, **243**, 695–715.
- Linn, C.E., Campbell, M.G. and Roelofs, W.L. (1987) Pheromone components and active spaces: what do moths smell and where do they smell it? *Science*, **237**, 650–652.



- Linster, C. (1993) Formal neural networks and olfaction: modeling pheromone discrimination in insects. Thèse de Doctorat, Université Pierre et Marie Curie, Paris.
- Linster, C., Masson, C., Kerszberg, M., Personnaz, L. and Dreyfus, G. (1993a) Computational diversity in a formal model of the insect olfactory macroglomerulus. *Neural Computation*, **5**, 239–252.
- Linster, C., Masson, C., Kerszberg, M., Personnaz, L. and Dreyfus, G. (1993b) Formal model of the insect olfactory macroglomerulus. In: Eeckman, F.H. and Bower, J.M. (eds), *Computation and Neural Systems*. Kluwer Academic Publishers, Boston, Dordrecht, London, 255–259.
- Linster, C., Marsan, D., Masson, C., Kerszberg, M., Dreyfus, G. and Personnaz, L. (1993c) A formal model of the insect olfactory macroglomerulus: simulations and analytical results. In: Giles, C.L., Hanson, S.J. and Cowan, J.D. (eds), *Advances in Neural Information Processing Systems*. San Mateo, Morgan Kaufmann Publications, 1022–1029.
- Linster, C., Kerszberg, M. and Masson, C. (1994a) Pheromone Detection, Ratio Discrimination and Oscillations: a new approach to olfactory coding. In Eeckman, F.H. (ed.), *Computation in Neurons and Neural Systems* Kluwer Academic Publishers, Boston, Dordrecht, London, 179–184.
- Linster, C., Kerszberg, M. and Masson, C. (1994b) How neurons may compute: the case of insect sexual pheromone discrimination. *Computational Neurosci.*, **1**, 231–238.
- Malun, D. (1991) Inventory and Distribution of Identified Uniglomerular Projection Neurons in the Antennal Lobe of *Periplaneta Americana*. *J. Neurobiol.*, **305**, 348–360.
- Masson, C. and Mustaparta, H. (1990) Chemical information processing in the olfactory system of insects. *Physiol. Rev.*, **70**, 199–245.
- Meredith, M.O. (1986) Patterned response to odor in Mammalian olfactory bulb: the influence of intensity. *J. Neurophysiol.*, **56**, 572–597.
- Olberg, R.M. (1983) Interneurons sensitive to female pheromone in the deutocerebrum of the male silkworm moth, *Bombyx mori*. *Physiol. Entomol.*, **8**, 419–428.
- Sun, X.J., Fonta, C. and Masson, C. (1993) Odour quality processing by bee antennal lobe interneurons. *Chem. Senses*, **18**, 355–377.

Received on December 15, 1994; accepted on August 18, 1995

## Appendix: Equations and simulation parameters

The probability  $P[x_i(t) = 1]$  that the state  $x_i(t)$  of neuron  $i$  at time  $t$  is 1 (firing):

$$P[x_i(t) = 1] = \frac{1}{1 + e^{-[v_i(t) - \Theta_i] / T}}$$

where  $v_i(t)$  is the evolution of the membrane potential:

$$v_i(t) = \left(1 - \frac{\Delta t}{\tau_i}\right) * v_i(t - \Delta t) + \frac{\Delta t}{\tau_i} * e_i(t)$$

with:

$$e_i(t) = \sum_j [w_{ij} * x_j(t - r_{ij})]$$

where  $w_{ij}$  is the weight ( $w_{ij} = \pm 1$ ) of the synapses between neuron  $j$  and neuron  $i$ , and  $r_{ij}$  is its delay (chosen randomly from uniform distributions).

Stimulation parameters:

$\tau = 80$  ms;  $r_{ij} = [5; 10]$  ms for afferent connections;  $r_{ij} = 100$  ms ( $\pm 10\%$ ) for inhibitory connections;  $r_{ij} = 20$  ms ( $\pm 10\%$ ) for excitatory connections;  $\Theta = 4.0$ ;  $T = 1.0$ .